

volume to 25 mL with 0.067 mol/L phosphate buffer, pH 6.8. The entire 25-mL volume was injected into a valve body using a programmable syringe drive. The filtered samples were washed with 5 mL of water and then lysed for ~ 20 s. After the lysis step, the material was forced through the filter by air pressure, and PCR was performed on aliquots of the filtered lysate. Typically, 100 μ L of filtered lysate was recovered.

All real-time fluorescence (RTF)-PCR reactions were performed using Cepheid SmartCycler[®] instrumentation and reaction tubes. The Mtb-specific primers and 6-carboxyfluorescein-labeled Molecular Beacon probes are described elsewhere (El-Hajj H, Marras SA, Tyagi S, Kramer FR, Alland D. A multiplex multi-colored Molecular Beacon assay for the rapid identification of *Mycobacterium tuberculosis* and rifampin resistance in clinical sputum samples, manuscript in preparation). Thermocycling conditions were 2 min at 95 °C, followed by 50 cycles of 10 s at 95 °C, 15 s at 58 °C, and 10 s at 72 °C. Fluorescence was measured during the 58 °C steps.

RTF-PCR results demonstrated the effectiveness of ultrasonic lysis for rupturing the BCG in the tube lysis system. When we used 10-fold serial dilutions of cultured cells, 14 CFU/100- μ L aliquot were detected. This demonstrated that ultrasonic lysis with silica beads was effective on BCG cells.

Serial 10-fold dilutions of BCG from 1480 to 0.015 CFU/mL were processed using the one-piece valve body and then analyzed by RTF-PCR.

The results for several of the samples, tested in duplicate, are shown in Fig. 1. Sample 1 is purified Mtb DNA (single result), sample 2 is 148 CFU/mL, sample 3 is 14.8 CFU/mL, and sample 6 is 0.015 CFU/mL. Samples with <14.8 CFU/mL were not detected in this series of experiments. Control experiments showed that ultrasonic lysis was required for DNA detection and that the NaOH solution was PCR-inhibitory.

These data from experiments using prototype filtration/lysis devices demonstrate the sample processing capabilities of the valve body component of the GeneXpert cartridge. The system effectively lyses BCG by use of ultrasonic energy and concentrates dilute, large volume samples by filtration. An additional advantage of the system is the ability to remove inhibitors of PCR by washing the captured sample. Removal of inhibitors will allow the use of current sputum digestant reagents, which will be important for comparison studies with culture and acid-fast bacteria staining methods of Mtb detection. The valve body is also capable of handling small or large sample volumes. These qualities are important for the range of applications planned for this system.

Release of detectable amounts of DNA without lysis was not observed. This implies that the system can concentrate and wash intact organisms, efficiently concentrating the target DNA after a subsequent lysis step. On the basis of the CFU calculations, a titer not detectable by PCR was concentrated to easily detectable concentrations.

Future efforts will investigate areas important for ana-

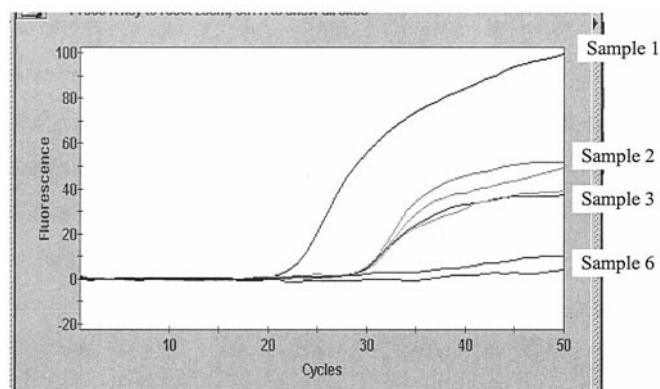


Fig. 1. RTF results for purified Mtb DNA (Sample 1), 148 CFU/mL BCG (Sample 2), 14.8 CFU/mL BCG (Sample 3), and 0.015 CFU/mL BCG (Sample 6).

lytical sensitivity and user requirements of rapid detection. Such areas will include filter surface area, pore size and material, valve body contained volume, fluid pumping rates, buffer composition, and ultrasonic lysis conditions, and other variables.

Finally, currently developed RTF multiplex PCR assays for Mtb single-nucleotide polymorphisms important in rifampin drug resistance will be adapted to the GeneXpert system. This may provide the final, critical technologic capability for the rapid, simultaneous, sensitive detection of Mtb and the presence of antibiotic resistance.

Technical assistance was provided by Molly Miranda, Rick Faeth, and Kristen Lloyd.

Magnetic Resonance Diagnostics: A New Technology for High-Throughput Clinical Diagnostics, David S. Wishart,¹ Lori M.M. Querengesser,^{2*} Brent A. Lefebvre,² Noah A. Epstein,² Russ Greiner,³ and Jack B. Newton² (¹ 2123 Dentistry/Pharmacy Center, Faculty of Pharmacy and Pharmaceutical Sciences, University of Alberta, Edmonton, Alberta, T6G 2N8 Canada; ²Chenomx Inc., 2007, 8308-114 Street, Edmonton, Alberta, T6G 2E1 Canada; ³ 122 Athabasca Hall, Artificial Intelligence Group, Department of Computing Science, University of Alberta, Edmonton, Alberta, T6G 2E8 Canada; * author for correspondence: fax 780-432-3388, e-mail lquerengesser@chenomx.com)

Magnetic resonance diagnostics (MRD) uses automated, high-throughput nuclear magnetic resonance (NMR) spectroscopy for the rapid identification and quantification of small-molecule metabolites in biofluid mixtures (blood, urine, saliva, cerebrospinal fluid, and others). Specifically, MRD involves using a high-field (400 MHz) NMR instrument equipped with a small-volume flow

probe and robotic sample handler to rapidly load biofluid samples and to collect their ^1H NMR spectra. Spectral deconvolution software automatically assigns individual peaks to particular compounds and calculates concentrations from peak areas. MRD uses the principle of chemical shift separation to physically separate and identify individual compounds directly from ^1H NMR spectra, thus avoiding chromatographic separation steps (e.g., HPLC, gas chromatography, and capillary electrophoresis). MRD is useful for rapid (<2 min per sample) qualitative and quantitative assessment of small-molecule metabolites.

NMR spectroscopy is not new to the field of clinical chemistry. Indeed several important applications have already been demonstrated in the area of diagnosis and therapeutic monitoring of metabolic disorders (1–4), in toxicologic and renal testing (5, 6), and in the profiling of blood lipoproteins and cholesterol (7). An emerging approach to enable high-throughput *in vivo* toxicology is called metabonomics, which uses high-resolution NMR to rapidly evaluate the metabolic status of an animal (8, 9).

A key limitation to all of these NMR approaches is that they depend on manual sample handling and/or manual (i.e., expert) spectral analysis. This has made most NMR approaches to clinical analyses far too slow or too costly for routine chemical profiling or high-throughput screening. Because MRD is fully automated (sample handling, spectral collection, and spectral analysis are all handled by robots or computers), this technique offers the potential for high-throughput, comprehensive, and inexpensive chemical analysis of a wide range of biofluid samples.

To demonstrate the potential of MRD for high-throughput clinical screening and metabolic profiling, we constructed a simulated test-run of 1000 urine samples processed by a prototype MRD instrument developed jointly by our laboratory and Varian Inc. (Palo Alto, CA). Our intent was to investigate the performance of the MRD instrument and software under the demands of a high-throughput clinical testing laboratory. The instrument was assessed on sample-processing speed, robustness of sample handling, and accuracy of identifying samples and compounds.

We followed protocols and conditions approved by the University of Alberta's Health Research Ethics Board to collect 1000 anonymous urine samples. A total of 925 samples were obtained from healthy adult volunteers who had completed consent forms. Seventy-five samples (63 children, 12 adults) were obtained as anonymous "discards" from several hospitals and clinics across Canada and were from patients with a wide variety of inborn errors of metabolism, neuroblastoma, and alcohol poisoning. All of the abnormal samples used in this test had been identified previously as such through conventional clinical screens. Among the abnormal samples were the following: 14 with propionic acidemia; 11 with methylmalonic aciduria; 11 with cystinuria; 6 with alkaptonuria; 4 with glutaric aciduria I; 3 each with pyruvate decarboxylase deficiency, ketosis, Hartnup disorder, cystinosis, neuroblastoma, phenylketonuria, ethanol toxicity, glycerol kinase deficiency, and hydroxymethylglutaryl-CoA-

lyase deficiency; and 2 with carbamoylphosphate synthetase deficiency.

For MRD analysis, 990- μL portions from each urine sample were transferred to 1.8-mL autosampler vials, to which 0.5 mmol/L (10 μL of a 50 mmol/L solution) 3-(trimethylsilyl)-1-propane-sulfonic acid, sodium salt (Sigma-Aldrich) was added. We manually adjusted the samples to pH 6.5 using $\text{HCl}_{(\text{aq})}$ or $\text{NaOH}_{(\text{aq})}$, as necessary. Manual pH adjustment was necessary because the software module required to automatically measure the pH and adjust the spectral deconvolution process was not completed in time for this study.

The prototype MRD instrument consisted of a 400 MHz Varian NMR spectrometer equipped with a 60- μL triple resonance-flow probe with an interchangeable flow cell and a modified Varian VAST (Versatile Automatic Sample Transport) system. The VAST system uses a robotic liquid handler (Gilson Model 215) and three computer-controlled switching valves, which direct sample flow to and from the flow probe through small-diameter Teflon tubing. Each urine sample (250 μL) was automatically loaded into the NMR spectrometer and a one-dimensional ^1H NMR spectrum collected (12 scans, 1.998 s; acquisition time, 0.5 s; acquisition delay, 6000 Hz sweepwidth) at ambient temperature ($21.5\text{ }^\circ\text{C} \pm 0.5\text{ }^\circ\text{C}$). After data collection, the urine sample was ejected and the flow probe extensively rinsed with distilled water before the next sample was loaded. Sample carryover was <1%.

NMR spectra were autoprocessed (e.g., transformed, phased, and referenced) and deconvolved with a suite of specially developed software applications and databases. The deconvolution process allows for the automated identification and quantification of components in biofluid mixtures through spectral database comparisons. We tested for 149 compounds currently contained in our spectral database.

The instrument automatically loaded and analyzed all 1000 samples in 35.2 h (1 sample every 2.1 min) with minimal human supervision. The mean sample loading and rinsing time was 93 s, whereas spectral acquisition had a mean of 32 s. The mean times for spectral processing and deconvolution (which can be performed in parallel with sample loading and data acquisition) were 7.1 and 72 s, respectively. During the test run, one sample-loading failure occurred, but did not lead to instrument downtime.

The deconvolution software was tested for accuracy for the following: (a) identification and quantification of urinary metabolites, (b) identification of nonpathologic and abnormal urine samples, and (c) identification of specific disease states or conditions. We evaluated compound-identification and/or -quantification accuracy primarily through detailed analysis of the abnormal samples. Specifically, the 15 disorders found in the abnormal urine samples were characterized by 34 unique or abnormally abundant metabolites (e.g., homogentisic acid, glycerol, glutaric acid, and others). Our results indicate that the MRD software succeeded in correctly identifying all 34 abnormal metabolites in all 75 abnormal samples. All 34

metabolites had been identified previously through conventional HPLC, gas chromatography–mass spectrometry, or amino acid or organic acid analysis. In some cases, these metabolites were also detected in nonpathologic urine samples, but at concentrations too low to be of significance or at concentrations well within the reference interval (10).

Although it was not possible to verify the MRD-measured concentrations for all metabolites (most conventional tests provide only qualitative results), our results for those metabolites that could be reliably quantified indicated a correlation coefficient between conventionally measured concentrations and MRD-measured concentrations of 0.99 (spanning a concentration range of 400 $\mu\text{mol/L}$ to 550 mmol/L). An example of compound identification and quantification achieved by this MRD software is shown in Fig. 1, which shows an abnormal urine NMR spectrum (specifically, methylmalonic aciduria), along with the MRD-calculated NMR spectrum. The calculated spectrum was generated from individual NMR spectra of MRD-identified and -quantified compounds.

Among nonpathologic urine samples, 87 ± 11 compounds were routinely identified and quantified by the MRD software on average. The identification and concentration of these metabolites were partially verified through manual spectral analysis of three randomly chosen samples and their subsequent chemical analysis. It was not practical to attempt to verify the identity of all compounds in the nonpathologic urine samples via conventional assays. The MRD software failed to consistently identify citrate, glycine, and histidine, probably because of the extreme sensitivity of their chemical shifts to pH and/or calcium ion concentrations.

A simple concentration-threshold algorithm achieved 96% sensitivity and 100% specificity, with 72 of 75 abnormal samples being detected and all 925 nonpathologic samples being correctly classified as nonpathologic. The three missed abnormal samples were cystinuria, glutaric aciduria, and carbamoylphosphate synthetase deficiency. This misclassification arose from the fact that these three samples exhibited relatively modest concentrations of abnormal metabolites. This particular algorithm compared MRD-quantified metabolite data with those values reported by Tietz (10), a database of “normal” and “abnormal” metabolite concentrations (both absolute and relative to creatinine) tabulated from several literature sources, as well as metabolite data collected from our own assays. Age- and gender-related adjustments were not included in the classification scheme.

Tests of the disease classification accuracy (for 1 healthy state and 15 diseases or conditions) yielded 95.5% and 92.4% for sensitivity and specificity, respectively. Interestingly, all false positives were confined to those urine samples already classified as abnormal. In particular, four false positives were identified for propionic aciduria, three false positives for phenylketonuria, two false positives were identified for cystinuria, and one false positive for ethanol toxicity. These classification problems likely arose from the age-independent, all-or-none classification

scheme used by our algorithm. A probabilistic assessment that included age- or gender-related values would likely have improved the results or revealed multiple disease possibilities.

Overall, this prototype instrument was rapid, robust, and accurate. It rapidly identified and quantified key metabolic markers of both common conditions (ethanol toxicity) and rare disorders (neuroblastoma). It appears to offer a high-throughput, inexpensive approach to metabolic profiling, with possible applications in medical

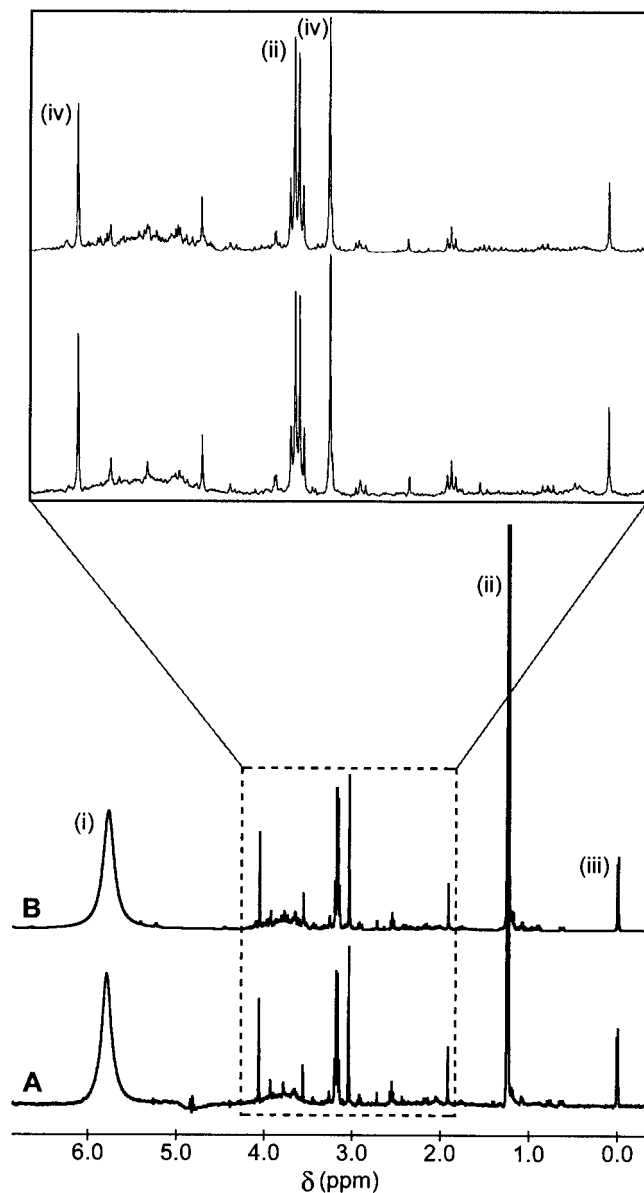


Fig. 1. NMR spectrum compared with software-generated spectrum. (A), ^1H NMR spectrum of a urine sample from a patient with methylmalonic aciduria. (B), calculated NMR spectrum derived from summing the individual spectra of the compounds and concentrations determined by the MRD software. (Inset), an enlargement of the region between 1.9 and 4.1 ppm. Peak labels are as follows: (i), urea; (ii), 2-methyl malonate; (iii), 2,2-dimethyl-2-silapentanesulfonic acid; (iv), creatinine.

diagnostics, drug compliance testing, toxicology, and food testing.

We wish to thank the University of Alberta Hospital, Toronto Hospital for Sick Children, Children's & Women's Health Centre of British Columbia, and Health Sciences Centre (Winnipeg, Manitoba) for contributing samples for this study. We also thank Dr. Fiona Bamforth (Department of Laboratory Medicine and Pathology, University of Alberta) for invaluable advice.

References

1. Lindon JC, Nicholson JK, Everett JR. NMR Spectroscopy of Biofluids. *Annu Rep NMR Spectrosc* 1999;38:1-88.
2. Wevers RA, Engelke UFH, Moolenaar SH, Brautigam C, De Jong JGN, Duran R, et al. $^2\text{H-NMR}$ spectroscopy of body fluids: inborn errors of purine and pyrimidine metabolism. *Clin Chem* 1999;45:539-48.
3. Bamforth FJ, Dorian V, Vallance H, Wishart DS. Diagnosis of inborn errors of metabolism using ^1H NMR spectroscopic analysis of urine. *J Inherit Metab Dis* 1999;22:297-301.
4. Burns SP, Woolf DA, Leonard JV, Iles RA. Investigation of urea cycle enzyme disorders by $^1\text{H-NMR}$ spectroscopy. *Clin Chim Acta* 1992;209:47-60.
5. Komoroski E M, Komoroski RA, Valentine JL, Pearce JM, Kearns GL. The use of nuclear magnetic resonance spectroscopy in the detection of drug intoxication. *J Anal Toxicol* 2000;24:180-7.
6. Foxall PJD, Mellotte GJ, Bending MR, Lindon JC, Nicholson JK. NMR spectroscopy as a novel approach to the monitoring of renal transplant function. *Kidney Int* 1993;43:234-45.
7. Freedman DS, Otvos JD, Jeyarajah EJ, Barboriak JJ, Anderson AJ, Walker JA. Relation of lipoprotein subclasses as measured by proton nuclear magnetic resonance spectroscopy to coronary artery disease. *Arterioscler Thromb Vasc Biol* 1998;18:1046-53.
8. Nicholson JK, Lindon JC, Holmes E. 'Metabonomics': understanding the metabolic responses of living systems to pathophysiological stimuli via multivariate statistical analysis of biological NMR spectroscopic data. *Xenobiotica* 1999;29:1181-9.
9. Robertson DG, Reilly MD, Sigler RE, Wells DF, Paterson DA, Braden TK. Metabonomics: evaluation of nuclear magnetic resonance (NMR) and pattern recognition technology for rapid in vivo screening of liver and kidney toxicants. *Toxicol Sci* 2000;57:326-37.
10. Tietz, NW, ed. *Clinical guide to laboratory tests*, 3rd ed. Philadelphia: WB Sanders Press, 1995:1-760.

The Use of Inosine 5'-Monophosphate Dehydrogenase (IMPDH) in the Development of a New Liquid Homogeneous Enzyme Immunoassay Technology, Allan R. Dorn,* Larry D. Mountain, Mitali Ghoshal, Raymond A. Hui, Lisa K. Klinedinst, Janice E. Rugaber, Andrew F. Schamerloh, and Salvatore J. Salamone (Roche Diagnostics Corporation, Centralized Diagnostics Business Unit, 9115 Hague Rd., PO Box 50457, Indianapolis, IN 46250-0457; * author for correspondence: fax 317-521-3085, e-mail allan.dorn@roche.com)

The objective of the present study was the development of a quantitative liquid homogeneous immunoassay specific for theophylline based on the specific uncompetitive inhibition of inosine 5'-monophosphate dehydrogenase (IMPDH) by mycophenolic acid (MPA). This was accomplished by covalent coupling of theophylline to MPA to form a theophylline-MPA conjugate (Fig. 1).

IMPDH (EC 1.1.1.205) (1) catalyzes the NAD-dependent oxidation of inosine 5'-monophosphate (IMP) to

xanthosine 5'-monophosphate (XMP). The enzyme follows an ordered Bi-Bi reaction sequence of substrate and cofactor binding and product release. In the first step, IMP binds to IMPDH, followed by the binding of the cofactor NAD. After IMP oxidation, the reduced cofactor, NADH, is released from IMPDH, followed by the release of XMP. To monitor the reaction, the rate of NADH formation is measured at 340 nm. Uncompetitive inhibition occurs when MPA combines with the IMPDH-XMP complex at the active site of the enzyme to form IMPDH-XMP-MPA complex, which is unable to release XMP. IMPDH inhibition depends only on the concentration of MPA because of the uncompetitive nature of inhibition by MPA. Thus, the greater the concentration of MPA inhibitor, the greater the inhibition of the enzyme. An uncompetitive inhibitor of IMPDH inhibits by binding at the active site of the enzyme and does not compete with IMP or NAD for inhibition of the enzyme. Increasing substrate concentration does not reverse this type of inhibition.

Two properties of MPA inhibition of IMPDH may facilitate the development of homogeneous enzyme immunoassays. The first property is that an uncompetitive inhibitor as a target conjugate is preferred over a competitive inhibitor because uncompetitive inhibitors are rare in nature and should be less susceptible to interferences from drugs and naturally occurring substances, which frequently are competitive inhibitors of enzymes. The second property is that the sensitivity of MPA inhibition ($K_i = 10 \text{ nmol/L}$) (2) favors its use in enzyme immunoassays.

We developed this homogeneous immunoassay by covalently attaching theophylline to a position on MPA that did not interfere with the uncompetitive inhibition of IMPDH. To assess the inhibition of IMPDH by the theophylline-MPA derivative, we measured the IC_{50} and

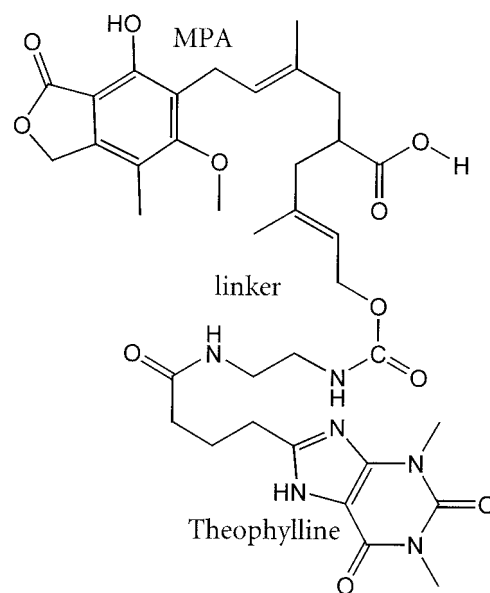


Fig. 1. Theophylline derivative of mycophenolic acid (MPA-5'-isoprenyl-theophylline).